# Supermultiplet classification of higher intrashell doubly excited states of $H^-$ and He

D. R. Herrick, M. E. Kellman,* and R. D. Poliak
*Chemistry Department and Institute of Theoretical Science, University of Oregon, Eugene, Oregon 97403*
(Received 6 March 1980)

We compute new estimates of energy levels of doubly excited states with two electrons in the same shell, for all principal quantum numbers $N \leq 5$ and angular momentum values $0 \leq L \leq 2N-2$ in $H^-$ and He. We investigate the structure of these intrashell spectra using a recent "supermultiplet" approach which originates in the O(4) shell structure of one-electron atoms. We provide new interpretations of the electron correlation underlying the O(4) states and supermultiplets of two-electron atoms; this accounts qualitatively for approximate separability of rotationlike and vibrationlike progressions of levels found in the computed spectra. Certain diamond-shaped patterns of supermultiplet energies are found to contain near degeneracies of levels with $\Delta L = \pm 2$; this accounts in part for level clustering we find in the unresolved spectra. Our investigation of scaling of the apparent rotational and vibrational parts of the energy with higher $N$ shows consistency with a simple model of the atom which has electrons on the surface of a spherical shell, with radius $R \simeq N^2$. We investigate the model group theoretically, and find two different O(4) groups which describe angular electron correlation in limiting cases of large or small shell radius for each principal quantum number $N$. A third O(4) group is related to intrashell radiative transitions.

## I. INTRODUCTION

A previous paper[1] described a novel supermultiplet approach for classifying doubly excited states of two-electron atoms with both electrons in the same shell. Those intrashell supermultiplets led to the discovery of very systematic progressions of apparent ro-vibrational energy levels in shells $N \leq 3$ in He. The purpose of the present paper is threefold. First, we have computed first estimates of all higher intrashell double-excitation levels $N \leq 5$ for both He and $H^-$. A description of double-excitation shell structure, symmetry classifications, and wave functions is given in Sec. II. Second, we give in Sec. III a clear exposition of the O(4) quantum numbers, wave functions, and generators underlying the supermultiplets. We also provide new physical interpretations of generators and quantum numbers that are related to the ro-vibrational level structure. Third, we investigate the supermultiplet structure of levels in Sec. IV; we describe near-degeneracies of certain levels, and scaling of ro-vibrational excitations with higher principal quantum number. We summarize these results in Sec. V. One of our goals is to present this material simply, so that persons previously unfamiliar with the language of the O(4) group may learn some of the basics of it here for doubly excited states. Reference 1 also suggested an alternate, "molecular" approach to the intrashell spectrum, involving floppy vibrations and rotations similar to those of a linear triatomic molecule. Here we will focus mainly on the group-theoretical approach. We will give the ro-vibrational interpretation and comparisons with spectra in other areas of physics and chemistry in a subsequent paper.[2]

## II. DESCRIPTION OF DOUBLY EXCITED STATES

Basic terminology for two-electron atoms is illustrated with He, which has a closed-shell ground-state configuration $1s1s$ which renders the atom chemically inert. Singly excited states lie below the first ionization threshold at 24.6 eV, and have configurations $1snl$ with one electron in a higher shell. This is indicated by the principal quantum number $n$, and the orbital angular momentum $l$. Doubly excited states lie above the first ionization threshold, and have configurations $n_1 l_1 n_2 l_2$ with $n_1, n_2 \geq 2$. The double-excitation regime extends from $2s2s$ at 57.9 eV, up to the threshold for double ionization at 79.0 eV. Most of these states are resonances in the single ionization continuum, and are described as quasibound states which decay by Coulomb autoionization. Successive ionization thresholds are labeled with a principal quantum number $N = 1, 2, \ldots$ for bound levels of the remaining ion: $He \rightarrow He^+(N) + e^-$. Doubly excited states below each of these thresholds are labeled with two principal quantum numbers $N$ and $n$, and fall into two types: (i) *intrashell states* with configurations $n = N$, and (ii) *intershell states* with configurations $n > N$. These levels may be distinguished by their behavior along the isoelectronic sequence, where in the limit $Z \rightarrow \infty$ the levels are those of independent electrons in degenerate hydrogenic orbitals. Doubly excited states are also classified with the usual term symbol $^{2S+1}L^{\pi}$ for the exact symmetries of the atom: $L$ for SO(3) rotation, $S$ for SU(2) spin, and $\pi$ for the parity.[3]

The difficulty in classifying doubly excited states further originates in electron correlation due to the Coulomb repulsion operator $1/r_{12}$. This breaks

 

the $SO(3)_1 \times SO(3)_2$ symmetry of single configurations from a central-field approximation, and thus leads to configuration mixing involving different values of $l_1$ and $l_2$. This manifests itself clearly in configuration-mixed channels[4] of intershell Rydberg series below ionization thresholds $N \geq 2$. Similar double-excitation channels in $H^-$ have a modified level structure, due to the absence of a long-range Coulomb attraction for the more-diffuse electron. Most previous numerical studies of doubly excited states with the Schrödinger equation have dealt with the classification of this channel structure, usually for only one value of $L$ at a time. The supermultiplets of Ref. 1 and the present work focus on the intrashell part of the spectrum for each shell $N$. The supermultiplets describe a very broad range of spectral systematics, because they take into account all of the values of $L$ at the same time.

Owing to the open-shell structure of doubly excited states, the electron correlation for the intrashell levels is in some ways similar to that found in the valence shell of a chemically reactive system. The configuration mixings thus relate to what may be called the "geometry" of intrashell electron pair correlation for an isolated atom.[5] Rigid geometries play a key role in molecular-structure theory, where at a simple level of approximation chemists describe bond angles using a hybridization of valence-shell atomic orbitals. Hybridization, which means "linear combination of orbitals with different $l$", thus breaks the SO(3) symmetry of one-electron atomic orbitals, and gives new orbitals directed towards other atoms for maximum bonding. This is illustrated by the orbital $s+\sqrt{3}p_z$, which describes the tetrahedral $sp^3$ hybridization. A linear $sp$ hybridization $s \pm p_z$ is perhaps more familiar to atomic physicists as the Stark-electric-field mixing of the degenerate $N=2$ level of H. The $l$ mixing that occurs in doubly excited states is analogous, and involves breaking of the one-electron SO(3) symmetry due to the noncentral field of $1/r_{12}$. The resulting configuration mixing allows a favorable correlation of the two electrons, usually described with the interelectronic angle $\theta_{12}$, subject of course to conservation of the total angular momentum of the atom. The notion of a geometry for the intrashell correlation is important for understanding the apparent ro-vibrational level structure we find embedded in the computed spectra.

Our present numerical estimates of doubly excited states use a modified version of a method for describing charge distributions for nonclosed-shell electron correlation in many-electron atoms.[6] Neglecting spin for the moment, we represent the open-shell structure of each double-excitation level $N$ with a wave function $\Psi_N$ which contains two orthogonal parts:

$$\Psi_N = \Phi + \chi , \tag{2.1}$$

chosen so that $\Phi$ is normalized to unity. Here $\Phi$ describes the near-degeneracy correlation included in the intrashell mixing of configurations $(Nl, Nl')$. The function $\chi$ represents additional open-shell correlation described by virtual pair excitations from configurations in $\Phi$ to other configurations of the type $(Nl'', Fl''')$. Each pair correlation radial function $F_l(r)$ is chosen orthogonal to the intrashell radial function $R_{Nl}(r)$; both of these radial functions are chosen orthogonal to hydrogenic radial functions $R^{\rm hyd}_{N'l}(r)$ for lower shells $N' < N$ in order to account for continuum stability of autoionizing states. The intrashell basis includes a finite number of orbitals $0 \leq l \leq N-1$, and hence a finite number of configurations in $\Phi$. Clebsch-Gordan coupling then gives the allowed values of the angular momentum for intrashell states: $0 \leq L \leq 2N-2$. Owing to the finite size of the intrashell basis, the number of configurations in $\chi$ is also finite. For each value of $N$ and $L$ the radial basis $F_l(r)$ includes only the values $0 \leq l \leq N-1+L$. Taking into account spin, we illustrate the configuration mixing structure of $\Psi_N$ for the case of $^1P^0$ intrashell states with $N=3$:

$$\begin{aligned}\Psi_3 = {} & a_0 |3s3p\,^1P^0) + a_1 |3p3d\,^1P^0) + c_0 |3sFp\,^1P^0) \\ & + c_1 |3pFs\,^1P^0) + c_2 |3pFd\,^1P^0) + c_3 |3dFp\,^1P^0) \\ & + c_4 |3dFf\,^1P^0) ,\end{aligned} \tag{2.2}$$

with intrashell mixing coefficients normalized to unity, $a_0^2 + a_1^2 = 1$.

We note that the function $\chi$ becomes similar to close-coupling[7] wave functions for two-electron atoms if we use hydrogenic radial functions in the intrashell basis. Oberoi[8] used a function similar to $\chi$ for low-$L$ states in the $N=3$ and $N=4$ shells, including nonlinear variations of orbitals. Our present estimates of $\Psi_N$ use a hydrogenic intrashell basis, and a finite expansion of radial functions in $\chi$ in terms of hydrogenic orbirals $N < n \leq 7$. Our linear approximation of $\Psi_N$ is thus similar to earlier hydrogenic configuration interaction for low $N$,[9] and gives intrashell energies comparable to Oberoi's,[8] and other configuration interaction including additional angular correlation.[10] Our calculations are the first ones for all intrashell levels $N \leq 5$.

One consequence of a finite linear variational approximation of $\Psi_N$ is the occurence of intrashell energy eigenvalues above each double-excitation autodetatchment threshold in $H^-$. Increasing basis size, or nonlinear variations of orbital exponents in the radial functions $F_l(r)$, would result in a col-

lapse of levels to threshold. It is possible, however, that some of the levels above threshold would continue to represent resonance states, as illustrated by the $^1P^0$ shape resonance above the $N=2$ threshold.[11] Very little is known about possible shape resonances for higher shells. We will tentatively include all of the intrashell energy eigenvalues in our computed spectra, at least until more accurate predictions of the stability of levels above threshold become available. One reason we choose to show them will be seen in Sec. IV, where we discuss a possible link of the instability to a ro-vibrational predissociation.

## III. O(4) MULTIPLET CLASSIFICATION

In this section we describe and interpret the O(4) quantum numbers that are used to construct the supermultiplets for intrashell energy levels in He and $H^-$. Since the O(4) approach is unfamiliar to most, we will give a fairly detailed account of the method, including some new results derived here. Previous work has indicated several useful ways that O(4) may be used to describe configuration interaction in two-electron atoms. These include degenerate intrashell hydrogenic orbital mixings at high $Z$,[12,13] intershell channel mixings at low $Z$ and $L$,[9,14,15] and intershell channel mixings at high $Z$ and $L$.[16] In our present computations the wave function $\Psi_N$ for each level in He and $H^-$ involves a substantial mixing of both intrashell ($\Phi$) and intershell ($\chi$) configurations. There are two ways of interpreting these results for the intrashell energy levels. The first method uses O(4) to describe intrashell configuration mixing at high $Z$, and then follows each level into the low-$Z$ regime. The second method uses O(4) to describe intershell channel mixings directly at low $Z$; intrashell levels are then identified as the lowest levels in channels. The former approach leads to two quantum numbers, $P$ and $T$, that form the basis of intrashell multiplets used for constructing $d$ supermultiplets in Ref. 1. The latter approach involves a related pair of quantum numbers, $K$ and $T$, for channels that underlie the $I$ supermultiplets of Ref. 1. As we will see, the two views emphasize different aspects of the electron correlation that are related to the ro-vibrational interpretation of supermultiplet levels. The organization of the rest of this section is as follows: Sec. III A summarizes properties of O(4) and the one-electron orbitals; Sec. III B describes the two-electron intrashell basis using three different O(4) subgroups; Sec. III C describes the intershell channel part of the wave function; and Sec. III D interprets the electron correlation in the intrashell states.

### A. Resume of O(4) and definition of symbols

The O(4) group is generated by the group of proper rotations in four dimensions, SO(4), plus reflections.[17] The SO(4) group has six Lie-algebra generators defined as components of vectors $\vec{l}$ and $\vec{b}$ which satisfy commutation relations

$$\begin{aligned} &[l_j, l_k] = i\epsilon_{jkm} l_m , \\ &[l_j, b_k] = i\epsilon_{jkm} b_m , \\ &[b_j, b_k] = i\epsilon_{jkm} l_m . \end{aligned} \tag{3.1}$$

Each irreducible representation of SO(4) may be labeled with two numbers $(p, q)$, with $p$ positive, $q$ positive or negative, and $p \geq q$. In our atomic applications $p$ and $q$ will always be integers. Individual states for the subgroup chain $SO(4) \supset SO(3) \supset SO(2)$ are then labeled with four numbers $p$, $q$, $l$, and $m$, contained in the eigenvalues of the Casimir invariants

$$\begin{aligned} &\vec{b}^2 + \vec{l}^2 = p(p+2) + q^2 , \\ &\vec{l} \cdot \vec{b} = q(p+1) , \\ &\vec{l}^2 = l(l+1) , \\ &l_z = m . \end{aligned} \tag{3.2}$$

A hierarchy for integer values of the numbers is

$$\begin{aligned} &p = 0, 1, 2, \ldots , \\ &q = p, p-1, \ldots , -p , \\ &l = p, p-1, \ldots , |q| , \\ &m = l, l-1, \ldots , -l . \end{aligned} \tag{3.3}$$

Thus each of the representations described by $(p, q)$ contains a multiplet of SO(3) terms with $|q| \leq l \leq p$. The total number of states in each representation is then given by the formula

$$g_{p,q} = (p+1)^2 - q^2 . \tag{3.4}$$

The reflection operation mixes the representations $(p, q)$ and $(p, -q)$. Together, this conjugate pair of SO(4) representations makes up a single irreducible representation of O(4), labeled here with the symbol $[p, |q|]$. When $q = 0$ the representation is self-conjugate, and each of the SO(3) states has a definite reflection symmetry. In our atomic applications we will label states in each representation according to their parity $\Pi$ for inversion of electronic coordinates. When $q = 0$ this satisfies $\Pi(-1)^l = +1$ for atomic wave functions. It is therefore natural to distinguish between two types of "multiplets" of states in each O(4) representation, according to the number

$$\eta = \Pi(-1)^l . \tag{3.5}$$

We label these multiplets $[p, |q|]^+$ or $[p, |q|]^-$ for states with the two types of parity $\eta = +1$ or $-1$,

respectively.

In the case of hydrogen atom orbitals,[18-20] the $N^2$-fold degeneracy of levels in each shell is explained by the SO(4) group generated by the orbital angular momentum $\vec{l}=\vec{r}\times\vec{p}$, and the energy-weighted Lenz vector

$$\vec{b}=N[\vec{p}(\vec{r}\cdot\vec{p})-\vec{r}(p^2-1/r)]\,. \tag{3.6}$$

Classically, these vectors describe the orientation of a planar Kepler orbit in space; $\vec{l}$ is perpendicular to the plane of the ellipse, while $\vec{b}$ lies along the major semiaxis. Quantum mechanically, the orthogonality of $\vec{l}$ and $\vec{b}$ means that $q=0$, and hence each degenerate manifold of hydrogen orbitals with $l=0,1,\ldots,N-1$ is contained in a single irreducible representation of SO(4) with $p=N-1$. Taking into account the parity of these states, this is the self-conjugate O(4) multiplet $[N-1,0]^+$.

There is a second way of representing the SO(4) states, that is related to the linear Stark effect in hydrogen. The electric field breaks the SO(3) symmetry of the atom, but the hydrogenic Stark states remain separable in parabolic coordinates. The group theoretical analog of the separability at zero field is a product group representation SO(4) = SU(2) × SU(2). Generators of the SU(2) groups are $\vec{F}=\frac{1}{2}(\vec{l}+\vec{b})$ and $\vec{G}=\frac{1}{2}(\vec{l}-\vec{b})$, with

$$\begin{aligned}&[F_j,F_k]=i\epsilon_{jkm}F_m\,,\\ &[G_j,G_k]=i\epsilon_{jkm}G_m\,,\\ &[F_j,G_k]=0\,.\end{aligned} \tag{3.7}$$

Generally for SO(4), these groups have Casimir invariants $\vec{F}^2=f(f+1)$ and $\vec{G}^2=g(g+1)$, which are related to previous labels by $p=f+g$ and $q=f-g$. The self-conjugacy of hydrogen-atom representations gives $f=g=\frac{1}{2}(N-1)$. Owing to the SO(2) symmetry of the electric field, $m$ is a good quantum number. The linear Stark energies are also described by the electric quantum number $k$, with $b_z=k$ in the hydrogen orbital basis.

Both types of SO(4) states are used in the classification of two-electron configuration mixings. SO(4) plays a similar role in both the one- and two-electron problems. In the hydrogen-atom Stark effect, neither SO(4) nor SO(3) describe an exact symmetry at nonzero field strength. Thus the electric quantum number $k$ only approximately classifies the states, which are quasibound resonances in the field ionization continuum. In doubly excited two-electron atoms the Coulomb interaction $1/r_{12}$ represents an internal field which breaks both the one-electron SO(4) and SO(3) symmetries; quantum numbers for coupled SO(4) representations thus only approximately classify the energy levels, which are quasibound resonances in the autoionization continuum.

### B. Coupled intrashell representations

We now describe coupled representations of SO(4) for intrashell states, corresponding to the near-degeneracy part $\Phi$ of the wave function. The two-electron product group $SO(4)_1\times SO(4)_2$ includes a total of 12 Lie-algebra generators; these may be coupled in several different ways, related to the coupling of four SU(2) angular momentum vectors in the Stark picture for one-electron orbitals. Our present approach uses generators which are symmetrized according to the permutation-inversion group for electrons in atoms; for two-electron atoms this is isomorphic with the point group $D_2$. Group elements include the identity, parity $\Pi$, exchange $P_{12}$ of spatial coordinates of two electrons, and the product operation

$$G=\Pi P_{12}\,. \tag{3.8}$$

Generators of the group $SO(4)_1\times SO(4)_2$ symmetrized according to irreducible representations of the permutation-inversion group are given with the character table in Table I. We define them here as

$$\begin{aligned}&\vec{L}=\vec{l}_1+\vec{l}_2\,,\quad \vec{D}=\vec{l}_1-\vec{l}_2\,,\\ &\vec{A}=\vec{b}_1+\vec{b}_2\,,\quad \vec{B}=\vec{b}_1-\vec{b}_2\,.\end{aligned} \tag{3.9}$$

$\vec{L}$ is the usual generator of SO(3) orbital angular momentum for two-electron atoms. Commutation relations of $\vec{L}$ with each of the other three vector operators, together with the appropriate reflection operations, lead us to consider three separate O(4) subgroups. These groups, and their generators, are labeled as follows: $O(4)_A$ with generators $\{\vec{L},\vec{A},G(\text{or }\Pi)\}$, $O(4)_B$ with generators $\{\vec{L},\vec{B},\Pi(\text{or }P_{12})\}$, and $O(4)_D$ with generators $\{\vec{L},\vec{D},P_{12}(\text{or }G)\}$. It is interesting to note that the group $O(4)_B$ generates maximal breaking of the permutation-inversion symmetry. We interpret generators of the three O(4) groups for intrashell states as follows:

(i) The group $O(4)_A$ includes the generator $\vec{A}$,

TABLE I. Character table for the permutation-inversion group for two-electron atoms. $G$ is defined in Eq. (3.8) as the product of parity ($\Pi$) and exchange ($P_{12}$). Also shown are transformation properties of generators of the group $SO(4)_1\times SO(4)_2$ for intrashell energy levels.

| | $E$ | $P_{12}$ | $\Pi$ | $G$ | Generator |
|---|---|---|---|---|---|
| $A_1$ | 1 | 1 | 1 | 1 | $\vec{l}_1+\vec{l}_2$ |
| $B_1$ | 1 | 1 | −1 | −1 | $\vec{b}_1+\vec{b}_2$ |
| $B_2$ | 1 | −1 | 1 | −1 | $\vec{l}_1-\vec{l}_2$ |
| $B_3$ | 1 | −1 | −1 | 1 | $\vec{b}_1-\vec{b}_2$ |

which leads to one type of configuration mixing in the two-electron basis. In the case of hydrogenic orbitals, intrashell matrix elements of one-electron radial vectors may be represented by $\vec{r} = (3N/2Z)\vec{b}$, and $\hat{r} = (1/N)\vec{b}$ for the unit vector.[15,20,21] In the two-electron basis then, $\vec{A}$ is directly related to intrashell matrix elements of the operator $\vec{r}_1 + \vec{r}_2$. The group $O(4)_A$ is therefore related to intrashell dipole radiative transitions, or Stark-effect mixings due to an electric field.

(ii) The group $O(4)_B$ leads to a second type of configuration mixing in the intrashell basis, since the generator $\vec{B}$ describes matrix elements of $\vec{r}_1 - \vec{r}_2$ or $\hat{r}_1 - \hat{r}_2$. The group is therefore related to the average spatial correlation of electrons in degenerate hydrogenic orbitals; the operator $\vec{L} \cdot \vec{B}$ describes the angular momentum about the average interelectronic axis. Reference 12 depicts two possible arrangements of classical Lenz vectors $\vec{b}_1$ and $\vec{b}_2$ corresponding to favorable and unfavorable electron correlation for a pair of Kepler orbits. The actual motions carried out by the classical vectors $\vec{b}_1$ and $\vec{b}_2$ are more difficult to depict, since they are complicated due to the Coulomb interaction $1/r_{12}$ and conservation of total angular momentum. As a result of the interaction, the Lenz vectors execute coupled precessional motion, which is presumably slower than the motion of each electron in its orbit. The angle between $\vec{b}_1$ and $\vec{b}_2$ is therefore related to the average interelectronic angle $\theta_{12}$. Three features of the motion of the Lenz vectors could account qualitatively for similar features in the intrashell doubly excited states. First, stretching motions of $\vec{b}_1$ and $\vec{b}_2$ which conserve one-electron energy necessarily give rise to changes in the one-electron angular momentum. In the quantum picture the one-electron generators satisfy $\vec{l}^2 + \vec{b}^2 = N^2 - 1$ for example. $l$ mixing of degenerate classical orbits is analogous to quantum-mechanical orbital hybridization, and hence to configuration mixing. Second, are coupled *rotational motions* of the Lenz vectors; these would include internal rotations about the axis $\vec{B}$. Third, are *bending motions* which change the angle between the Lenz vectors. It is possible that numerical studies of classical trajectories would show coupled motions similar to the ones we have described. Rotations and vibrations of the Lenz vectors are at least qualitatively consistent with the ro-vibrational level structure found in the supermultiplet spectra.[1]

(iii) The third intrashell group $O(4)_D$ does not describe configuration mixing, because the generators $\vec{L}$ and $\vec{D}$ both commute with the one-electron SO(3) invariants $\vec{l}_1^2$ and $\vec{l}_2^2$. The two invariants of $O(4)_D$ may be seen in the centrifugal part of the two-electron kinetic energy:

$$\vec{l}_1^2/r_1^2 + \vec{l}_2^2/r_2^2 = \tfrac{1}{4}(\vec{L}^2 + \vec{D}^2)(1/r_1^2 + 1/r_2^2) + \tfrac{1}{2}(\vec{L} \cdot \vec{D})(1/r_1^2 - 1/r_2^2). \quad (3.10)$$

Notice that the operator $\vec{L} \cdot \vec{D}$ allows coupling of symmetric and antisymmetric radial coordinates, such as $r_1 + r_2$ and $r_1 - r_2$. It is the only part of the two-electron energy which couples these degrees of freedom directly. In this sense it plays a role analogous to the Coriolis interaction in a linear triatomic molecule; the Coriolis force due to rotation and bending vibration excites the asymmetric stretch vibration of the molecule.

The preceding interpretation of $O(4)_D$ is independent of the radial part of the intrashell basis. In contrast, the interpretations of the groups $O(4)_A$ and $O(4)_B$ were directly linked to the degenerate hydrogenic orbital basis. Similar, approximate interpretations of these groups would be expected in other orbital bases, such as Hartree-Fock type functions at low $Z$ in the two-electron isoelectronic series.

Thus far, we have interpreted only the Lie-algebra generators for the three O(4) groups defined on the intrashell configuration basis. We now describe the relationship between the irreducible representations of these groups. There has been some confusion in the past as to the proper identification of coupled states for two electrons. Initial work in this area misidentified the group we call $O(4)_A$ as the one for configuration mixings due to $1/r_{12}$ (Ref. 22). Subsequent work pointed out that the group $O(4)_B$ is actually the one to use for two electrons.[12,13] Pairwise coupling of invariants for $O(4)_B$ was also used[23] to describe configuration mixing in first-row many-electron atoms. Here we will describe two-electron couplings in the intrashell basis; we give some additional details of the intrashell symmetry breaking of $SO(4)_1 \times SO(4)_2$ in the Appendix.

We distinguish between three SO(4) bases for the intrashell states. The first is the single-configuration representation, which according to the group $O(4)_D$ would have states labeled

$$|pqLM)_D = |(Nl_1Nl_2')LM), \quad (3.11)$$

with $p = l + l'$ and $q = l - l'$. We use a similar symbol $|pqLM)_A$ to label states for the group $O(4)_A$. Our main interest is with the basis which diagonalizes $O(4)_B$ Casimir invariants $\vec{L}^2 + \vec{B}^2 = P(P+2) + Q^2$ and $\vec{L} \cdot \vec{B} = Q(P+1)$; this we denote by $|PQLM)$, without a subscript. From the theory of angular momentum recoupling we find that the three bases are related by the following linear transformations:

$$|PQLM) = \sum_{p,q} |pqLM)_D (pqL|PQL), \quad (3.12)$$

$$|PQLM) = (-1)^c \sum_{p,q} |pqLM)_A (pqL|PQL), \tag{3.13}$$

$$|p'q'LM)_A = \sum_{p,q} |pqLM)_D (pqL|p'q'L)(-1)^{(p-q)/2}. \tag{3.14}$$

Here the phase factor is given by $c = N - 1 - \frac{1}{2}(P-Q)$, and the coupling coefficient is defined in terms of a 9-$j$ symbol as

$$(pqL|PQL) = (-1)^{(p-q)/2}[(p+q+1)(p-q+1)(P+Q+1)(P-Q+1)]^{1/2} \times \begin{Bmatrix} \frac{1}{2}(N-1) & \frac{1}{2}(N-1) & \frac{1}{2}(P+Q) \\ \frac{1}{2}(N-1) & \frac{1}{2}(N-1) & \frac{1}{2}(P-Q) \\ \frac{1}{2}(p+q) & \frac{1}{2}(p-q) & L \end{Bmatrix}. \tag{3.15}$$

As indicated in Eq. (3.12), the state $|PQLM)$ has a configuration-mixed structure; we denote the corresponding spatial wave function for intrashell SO(4) states by the symbol $\Phi_{PQLM}$. We find the SO(4) wave functions have the following properties under permutation-inversion operations:

$$\Pi \Phi_{PQLM} = (-1)^{L+Q} \Phi_{P-QLM}, \tag{3.16}$$

$$P_{12} \Phi_{PQLM} = (-1)^L \Phi_{P-QLM}, \tag{3.17}$$

$$G \Phi_{PQLM} = (-1)^Q \Phi_{PQLM}, \tag{3.18}$$

and time reversal:

$$\Phi^*_{PQLM} = (-1)^{Q+M} \Phi_{P-QL-M}. \tag{3.19}$$

In all cases we consider, $P$ and $Q$ are integers and satisfy $(-1)^{P+Q} = 1$. From Eqs. (3.18) and (3.8) we see then that the product of permutation-inversion quantum numbers satisfies $\Pi P_{12} = (-1)^Q$. Thus $G$ produces an effect on the SO(4) wave function analogous to that of a 180° rotation about an internal body-fixed axis. This rotation is realized with the operator $\exp(i\alpha \vec{L} \cdot \vec{B})$ within each SO(4) irreducible representation, when the rotation angle is chosen to be $\alpha = \pi/(P+1)$ radians.

When $Q = 0$ the parity of each SO(4) state satisfies $\Pi(-1)^L = +1$, and hence these states belong to self-conjugate O(4) multiplets $[P,0]^+$ with $\eta = +1$. Normalized wave functions for the O(4) multiplets $[P,T]^\eta$ with $\eta = \pm 1$ are given by the following linear combination when $Q \neq 0$:

$$\Phi^\eta_{PTLM} = (\Phi_{PTLM} + \eta(-1)^T \Phi_{P-TLM})/\sqrt{2}, \tag{3.20}$$

where we have used the number

$$T = |Q|. \tag{3.21}$$

The values of $P$ and $T$ are given by the Clebsch-Gordan series for the product representation, which may be seen from general results[17] to have the following form for intrashell states of two-electron atoms:

$$[N-1,0]_1 \times [N-1,0]_2 = \sum_{P,T} [P,T], \tag{3.22}$$

including only the following values of $P$ and $T$:

$$T = 0, 1, \ldots, N-1, \qquad P = T, T+2, \ldots, 2N-2-T. \tag{3.23}$$

We illustrate Eq. (3.22) for the case when two electrons occupy $2s$ and $2p$ orbitals in the $N=2$ shell,

$$[1,0]_1 \times [1,0]_2 = [0,0] + [2,0] + [1,1]. \tag{3.24}$$

This includes one $S$ term, plus $S$, $P$, $D$ terms, plus two $P$ terms, in three O(4) representations respectively; this gives $1+9+6=16$ states in all.

Our use of Eq. (3.12) for configuration mixings in doubly excited states involves a definite phase convention for the one-electron orbitals. Following an earlier convention[15] for matrix elements of generators we use the Condon-Shortley phase for angular momentum,[24] and radial functions which have the phase $(-1)^l$ at small $r$ near the nucleus. This radial phase is important, because it means that all one-electron radial functions have the same phase $(-1)^{N-1}$ at large values of $r$, on account of the $N-l-1$ nodes in each orbital. Consequently, the SO(4) configuration-mixing coefficients describe mostly angular correlation of the two electrons, at least to the extent that radial functions are similar in the region of peak radial density for intrashell states.

### C. Intershell channels

Section III B discussed the problem of $SO(4)_1 \times SO(4)_2$ coupling for intrashell configurations. This part of the wave function dominates at very high $Z$ in the isoelectronic series, where the hydrogenic-independent-particle picture is good. At low $Z$, the hydrogenic configuration interaction matrix includes substantial coupling between different shells; in the wave function $\Psi_N$ this is described by the function $\chi$, which for intershell channels controls the binding of the more radially diffuse electron below threshold. The classifica-

tion of these channels is important in our supermultiplet classification of intrashell energy levels. Following a procedure developed in Ref. 9, we first label channels using two quantum numbers $K$ and $T$. We then use the intrashell O(4) to tell us where to look in the channel spectrum for intrashell states. In this way we efficiently unravel the intrashell supermultiplets from the overlapping intershell spectrum. The intershell mixings also affect the distribution of $\theta_{12}$ for states in the supermultiplets, and are thus important to our interpretation of ro-vibrational energy-level structure. In a perturbation approach at high $Z$, these intershell mixings would contribute terms second order and higher in the energy.

Neglecting exchange for intershell states, the channel quantum number $K$ is seen in the following O(4) reduction of the product basis when $n \geq N$:

$$[N-1,0]_1 \times [n-1,0]_2 = \sum_{K,T} [n-1+K,T]\,. \tag{3.25}$$

The usual O(4) quantum number $P = n-1+K$ is not a very good label for intershell channels, because it changes value between successive states in the series for higher $n$. $K$, on the other hand, remains constant within a channel. In the hydrogenic configuration interaction matrix for low-lying levels in each shell, this separation of states with different values of $K$ and $T$ is seen as an approximate block diagonalization of the energy. Thus the classification with $K$ is much stronger than a classification based on the contribution of intrashell configurations alone. Nonetheless, it is still convenient to label the intrashell levels according to the quantum numbers $P$ and $T$ from the high-$Z$ limit.

The supermultiplet classification of intrashell states uses both types of quantum numbers. Figure 1 shows the values of $K$ and $T$ for all shells $N \leq 5$. The channel $K = N-1$, $T = 0$ is placed at the bottom of each of these diamond-shaped patterns, because it represents the most favorable correlation of the electrons. The values of $L$ in each channel may be visualized as rising vertically out of the plane of Fig. 1. A hierarchy for these quantum numbers is

$$\begin{aligned} &N = 1,2,3,\ldots\,,\\ &K = N-1, N-2, \ldots, 1-N,\\ &T = N-1-|K|, N-3-|K|, \ldots, 1 \text{ or } 0,\\ &L = T, T+1, T+2, \ldots\,. \end{aligned} \tag{3.26}$$

These channels are also labeled according to the two types of parity, $\eta = \pm 1$. Note in Eq. (3.26) that each channel described by $K$ and $T$ contains an infinite number of values of $L$. Above threshold, the channels for very high $L$ are related to large-impact-parameter scattering for systems such as $e^- + \mathrm{H}(N)$; these high values of $L$ are therefore not important in our treatment of intrashell levels. Instead, the values of $L$ are cut off for intrashell states in each channel. In the O(4) shell model the cutoffs are implicit in Eq. (3.25) when $n = N$, in which case $P = N-1+K$ for intrashell states. We therefore have two ways of viewing the spectrum of intrashell O(4) quantum numbers. The first way was described above in Sec. III B using $P$, $T$, and $L$. The second way starts with the channel quantum numbers $K$, $T$, and $L$ in Eq. (3.26), but modifies this to account for the finite restriction on intrashell angular momentum:

$$L = T, T+1, T+2, \ldots, N-1+K\,. \tag{3.27}$$

The two hierarchies of quantum numbers are related to the two types of O(4) quantum numbers discussed in Sec. III A. $P$, $T$, and $L$ are labels for the subgroup chain $\mathrm{O}(4) \supset \mathrm{O}(3)$. $K$ and $T$, on the other hand, originate in the $\mathrm{SU}(2) \times \mathrm{SU}(2)$ Stark-effect picture for the hydrogen atom. Herrick[15]

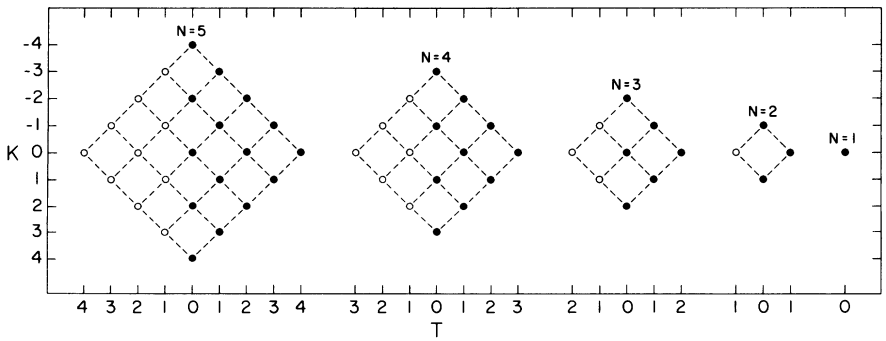


FIG. 1. Values of Stark-type O(4) quantum numbers $K$ and $T$ for channels below each one-electron threshold $N \leq 5$; double-excitation channels correspond to $N \geq 2$. Channels are separated into the two parity classes $\eta = +1$, shown with a filled circle, and $\eta = -1$, shown with an open circle; $\eta$ is defined in Eq. (3.5).

has investigated the connection between the two sets of quantum numbers using a dipole approximation[25] for the configuration mixing of intershell states. Since this picture of the atom bears on our interpretation of ro-vibrational types of correlation in the doubly excited states, we will briefly describe it here.

The method starts with a wave function similar to the function $\chi$ we discussed in Sec. II. After taking into account configuration mixing (including only the dipole term from $1/r_{12}$), and averaging over all degrees of freedom except the asymptotic radial coordinate $r_2 \gg r_1$, one is left with a set of decoupled radial equations

$$\left(\frac{d^2}{dr_2^2} - \frac{A}{r_2^2} + \frac{2(Z-1)}{r_2} + 2\epsilon\right) F_A(r_2) = 0 . \quad (3.28)$$

Here $\epsilon$ is the energy of the electron relative to the threshold for level $N$. Each channel is described with a different eigenvalue $A$ of the matrix of an effective centrifugal operator $l_2(l_2+1)+2r_1\cos\theta_{12}$ for each shell. In an O(4) representation the dipole channels are described by eigenvalues of two commuting channel invariants[15]:

$$\begin{aligned} \hat{A} &= (3N/Z)\vec{b}_1 \cdot \hat{r}_2 + \vec{l}_2^{\,2} , \\ \hat{W} &= \vec{L} \cdot [(3N/Z)\hat{r}_2 - 2\vec{b}_1] , \end{aligned} \quad (3.29)$$

in which $\hat{r}$ is the unit vector. Eigenvalues of these invariants describe configuration-mixed channels, and replace the single-configuration quantum numbers $l_1$ and $l_2$ over the entire isoelectronic series. At very low $Z$, the invariants describe a Stark-effect mixing of the degenerate manifold of bound states in level $N$, relative to the frame of the asymptotic electron. $K$ is the related electric quantum number, while $Q$ is the angular momentum quantum number for the body-fixed field axis. We again use $T = |Q|$ for the magnitude of the angular momentum projection, because parity mixes the conjugate states $\pm Q$ for two electrons. The behavior of the channel invariants at low $Z$ is seen in a perturbation expansion of their eigenvalues[15]:

$$\begin{aligned} A &= -(3N/Z)K + L(L+1) \\ &\quad + \tfrac{1}{2}(N^2 - 1 - K^2 - 3Q^2) + \cdots , \\ W &= -Q[(3N/Z) + 2K + \cdots] . \end{aligned} \quad (3.30)$$

The first term in the expansion of $A$ gives a Stark-level pattern like the channels shown in Fig. 1; the most favorable electron correlation in this Stark dipole approximation obtains when $K = N-1$. A fuller interpretation of the electron correlation in the channels will be given in Sec. III D.

### D. Ro-vibrational interpretation of correlated states

In Secs. III B and III C we described correlated wave functions originating in the SO(4) shell structure. The distributions of $\theta_{12}$ in our computed wave functions are similar to the ones for SO(4) states in two respects. First, our wave functions contain intrashell configuration mixings due to $1/r_{12}$; these are well-approximated by the SO(4) mixings. Second, the $K, T$ channel classification is generally very strong in the computed wave functions, and the intershell configurations in $\chi$ contribute correlation effects similar to those found in the Stark dipole channels at low $Z$. It is therefore important to understand at least qualitatively the differences between these types of correlation, and their relationship to possible ro-vibrational collective motion.

Rehmus *et al.*[26] have investigated SO(4) distributions for the interelectronic angle $\theta_{12}$ in a hydrogenic orbital basis. They found the distribution for the $^1S^e$ intrashell SO(4) wave function peaked in the region $\theta_{12} = 180°$ in each shell. This interpretation was the basis of our initial investigation of rotor-like series in the intrashell spectra of He and $H^-$.[27] The fact that Rehmus *et al.* had to resort to numerical studies of the SO(4) wave functions attests to the difficulty of this problem. Differences in the distributions for other values of $P$, $Q$, and $L$ are reflected in the average value $\langle\cos\theta_{12}\rangle$ for each of the states. In the Appendix we show how to derive the following expression for the intrashell SO(4) states using hydrogenic orbitals:

$$\langle\cos\theta_{12}\rangle = [4N^2 - 4 - 3P(P+2) - 3Q^2 + 2L(L+1)]/8N^2 . \quad (3.31)$$

We interpret this result using an average correlation angle defined by the inverse of Eq. (3.31), $\theta_e = \cos^{-1}\langle\cos\theta_{12}\rangle$. This is also related to the angle between two Lenz vectors $\vec{b}_1$ and $\vec{b}_2$, as we discussed in Sec. III B. There are two trends seen in Eq. (3.31) which relate to the problem of ro-vibrational collective excitations. First, within each SO(4) representation $(P, Q)$ increasing $L$ gives smaller values of $\theta_e$, and hence higher energies. The second trend relates to the $K, T$ picture of the intrashell states. For fixed $T$ and $L$, decreasing the value of $K$ in each of the diamond-shaped patterns in Fig. 1 gives smaller values of $\theta_e$, and hence higher energies. The first trend is related to collective rotational excitation of the system, while the second trend is related to vibrationlike excitations involving the angle $\theta_{12}$. With increasing $N$ the distribution of correlation angles is found to have a range of values $60° \leq \theta_e \leq 180°$ for $1-N \leq K \leq N-1$, respectively. This is consistent with a picture of favorable electron correlation in the SO(4) states, which tend to keep the electrons away from the Coulomb singularity at $\theta_{12} = 0°$.

Similar interpretations for collective rotational and vibrationlike motions are implicit in the level

structure of the eigenvalues of $A$ in Eq. (3.30) for dipole channels. The distribution of correlation angles for the intershell channels is more diffuse than it was for intrashell states, however, due to the fact that one of the electrons is farther from the nucleus. In a Stark approximation of the channels at low $Z$, the angular distribution gives $0^\circ \leq \theta_e \leq 180^\circ$ for $1-N \leq K \leq N-1$. In wave functions of low-lying intrashell levels then, admixtures of intershell configurations would reinforce the ro-vibrational picture, since the values of $\theta_e$ are near $180^\circ$ in both cases. In contrast to this, admixtures of intershell configurations in $\Psi_N$ for higher intrashell levels, and in particular those with $K<0$ or very high $L$, would involve very floppy collective motions. This is the regime where a simple rotor-vibrator picture is least applicable for intrashell states.[1] It is also the regime where intershell levels in $H^-$ are no longer stable, due to the fact that the centrifugal potential in Eq. (3.28) is repulsive. This long-range repulsion is the reason for the instability of certain eigenvalues in the $H^-$ spectrum, as discussed in Sec. II.

## IV. SUPERMULTIPLET CLASSIFICATION OF ENERGY LEVELS

In Sec. III we described O(4) multiplets, and gave interpretations of the electron correlation for related configuration-mixed wave functions. We now use those results, together with the prescription of Ref. 1, in order to construct and interpret the supermultiplet energy level structure in our spectra of He and $H^-$ for $N \leq 5$. Sections IV A and IV B illustrate the detailed structure of $I$ supermultiplets and $d$ supermultiplets, respectively, for the $N=4$ shell. This parallels the supermultiplet classification of the $N=3$ shell in Ref. 1. In Sec. IV C we give a description of the full intrashell spectrum for $N \leq 5$. We then investigate the approximate separability of the ro-vibrational levels in Sec. IV D.

### A. $I$ supermultiplets

This first type of supermultiplet emphasizes the description of intrashell states with $K$ and $T$ quantum numbers, which were illustrated in Fig. 1. The values of $L$ for each channel are then described with the quantum number

$$I = L - T = 0, 1, \ldots, 2N-2, \tag{3.32}$$

which gives the degree of rotational excitation relative to the lowest value of $L$ in each O(4) multiplet $[N-1+K, T]$. We thus obtain a similar diamond-shaped "$I$ supermultiplet" for each value of $I$; the size of these "diamonds" decreases with higher $I$ due to the cutoffs for the intrashell angular momentum.

Figure 2 gives the $I$ supermultiplet decomposition of term symbols for intrashell levels when $N=4$. Conjugate pairs of terms with the same values of $K$ and $T$ are arranged so that terms with $\eta=+1$ appear on the right-hand side of each supermultiplet. Within each $I$ supermultiplet then, levels having the same quantum numbers $T$ and $\eta$ have the same term symbol. Similar progressions of supermultiplets are easily constructed for other values of $N$; the ones for $N=3$ were shown in Ref. 1.

Figure 3 shows our $I$ supermultiplet classification of intrashell energies for $N=4$ levels of $H^-$, He, and $Z=\infty$. The high-$Z$ values were obtained by diagonalization of $1/r_{12}$ in the intrashell hydrogenic orbital basis. The unresolved spectra are shown at the left. Overall, the supermultiplets have a more ordered appearance at lower $Z$. Recall, however, that levels above threshold in $H^-$ may only be stable in the linear configuration ex-

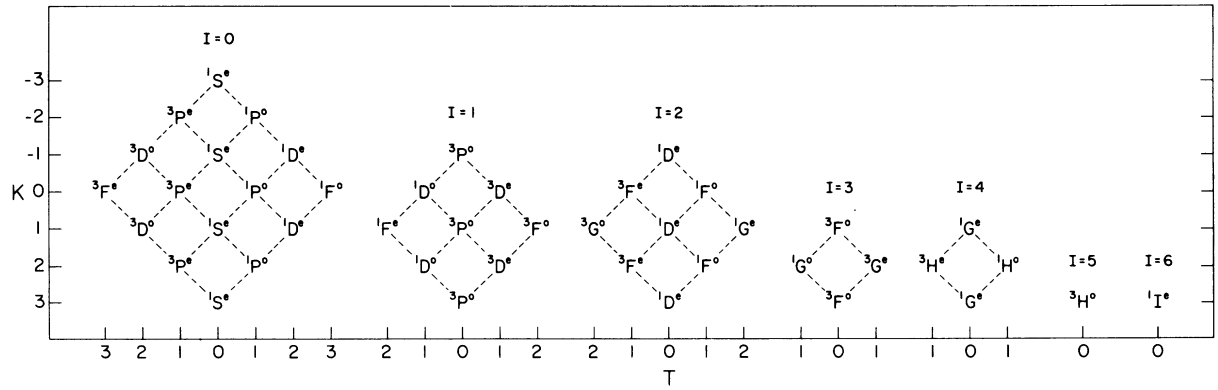


FIG. 2. $I$-supermultiplet, or "diamond" classification of term symbols for intrashell doubly excited states in the $N=4$ level. Each diamond supermultiplet has constituent terms with the same value of $I=L-T$, representing the degree of rotational excitation relative to the $K,T$ channels in Fig. 1. The lines between levels in each supermultiplet are used to identify similar levels in the energy spectra of Fig. 3.

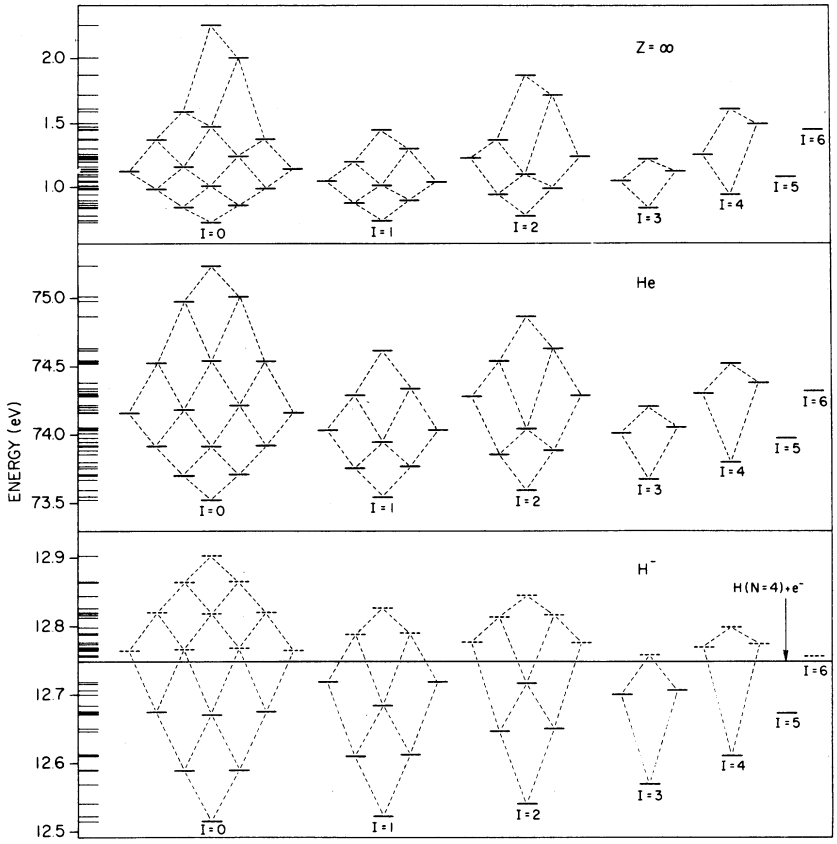


FIG. 3. $I$-supermultiplet classification of computed intrashell spectra for $N=4$ levels in $H^-$, He, and $Z=\infty$ (hydrogenic); illustrating isoelectronic behavior. Term symbols for levels were shown in Fig. 2. Note the approximate near-degeneracy of levels in the largest diamond; unresolved level clustering is shown at the left.

pansion approach we have used; they may collapse to threshold—or in some cases drop below threshold—when nonlinear variations of radial functions are taken into account. We note especially the nearly equal spacing of levels in the largest supermultiplet, $I=0$, as well as the near-degeneracy of levels with the same quantum number $K$. Each diamond has an approximate left-right symmetry originating in the accidental near-degeneracy of conjugate pairs of O(4) terms. The splitting of these levels was called "$T$ doubling" in Ref. 1. Here we also find that $T$ doubling tends to give levels with $\eta=-1$ lower in energy relative to the conjugate level with $\eta=+1$. The near-degeneracies (including $T$ doubling) weaken at higher values of $I$ in the supermultiplet spectrum. The number of levels in $I$ supermultiplets are contained in the sequences $1,4,9,\ldots,N^2$ for even $I$, and $1,4,9,\ldots,(N-1)^2$ for odd $I$; this gives a total of $\frac{1}{3}N(2N^2+1)$ levels for each shell.

### B. $d$ supermultiplets

The second type of supermultiplet emphasizes the intrashell O(4) picture. Each $d$ supermultiplet is made up from intrashell O(4) multiplets $[P,T]$ having the same value of $d\equiv\frac{1}{2}(P+T)$. In this way the O(4) product representation has an intermediate form[1]

$$[N-1,0]_1\times[N-1,0]_2=\{0\}+\{1\}+\cdots+\{N-1\}, \tag{4.1}$$

with each $d$ supermultiplet of intrashell states having an O(4) reduction

$$\{d\}=[2d,0]+[2d-1,1]+\cdots+[d,d]\,. \tag{4.2}$$

Each of these $d$ supermultiplets separates further into the two parity classes, labeled by $\{d\}^\eta$. There are a total of $(2d+1)(d+1)^2$ states in $\{d\}^+$, and $(2d+1)d^2$ states in $\{d\}^-$. The respective numbers of energy levels in these supermultiplets are

$(d+1)^2$ for $\{d\}^+$, and $d^2$ for $\{d\}^-$. Further clarification of the mathematical properties of the $d$ supermultiplets is needed. The multiplicities suggest that each $d$ supermultiplet may be reducible under a group SU(2)×SO(4), but we have been unable to identify a set of coordinates which would give such a separation in the wave function for doubly excited states. As noted earlier in Ref. 1, the $d$ supermultiplets are also related to an unusual SU(2) group generated by an operator $\vec{J}_>$ which is the larger magnitude vector of the more conventional SU(2) generators $\vec{j}=\frac{1}{2}(\vec{L}+\vec{B})$ and $\vec{k}=\frac{1}{2}(\vec{L}-\vec{B})$. These are related to the one-electron hydrogenic Stark SU(2) generators $\vec{F}$ and $\vec{G}$ as follows: $\vec{j}=\vec{F}_1+\vec{G}_2$ and $\vec{k}=\vec{F}_2+\vec{G}_1$. The quantum number $d$ is then associated with the larger of these vectors, with $\vec{J}_>^2=d(d+1)$. The hierarchy of intrashell quantum numbers $N, d, Q$ is similar to the usual spherical quantum numbers $N, l, m$ for the hydrogen atom:

$$N=1,2,\ldots,$$
$$d=0,1,\ldots,N-1, \tag{4.3}$$
$$Q=d,d-1,\ldots,-d.$$

Figure 4 gives the term symbol supermultiplets for $d\leq 4$, which allows one to construct the intrashell $d$ supermultiplets for levels $N\leq 5$. We have arranged each supermultiplet so that an O(4) multiplet $[P,T]^+$ appears on the right-hand side, while the conjugate multiplet $[P,T]^-$ is on the left-hand side. The parity and spin of levels in each O(4) multiplet alternate with increasing $L$, due to the fact that the generator $\vec{B}$ breaks these symmetries. Levels along the lower edges of $d$ supermultiplets have $L=T$, and thus belong to the same $I$ supermultiplet $I=0$. Our arrangement of $d$ supermultiplets in Fig. 4 reflects the approximate degeneracy of levels with the same value of $K$ in the largest $I$ supermultiplet for each shell.

Figure 5 shows our $d$-supermultiplet classification of intrashell energies for $N=4$ levels. These are the same energies shown in Fig. 3 using $I$ supermultiplets. The $d$ supermultiplets give an even more ordered and compact spectrum than the $I$ supermultiplets. Owing to the large number of levels, we show only the spectroscopic symbol for states with the same value of $L$, connected by lines similar to the ones in the more detailed representation of term symbols in Fig. 4. Energies tend to increase with $L$ in each O(4) multiplet, and the largest series $[6,0]^+$ is the one most like a cutoff rigid rotor spectrum.[27] Note that the multiplet $[2,0]^+$ for $Z=\infty$ has the level $^3P^o$ below the $^1S^e$ level however. The same $^3P^o$ level lies above $^1S^e$ in the spectra of He and $H^-$. This illustrates the apparently stronger, more rigid electron correlation at lower $Z$ in the isoelectronic series. We find similar inversions from a rotor ordering of levels in the $N=5$ shell.

### C. Levels for $N\leq 5$ in He and $H^-$

We show only the largest $I$ supermultiplet for each shell, to illustrate the interesting pattern of near-degeneracies we find in our computed spectra. These are shown in Fig. 6, which includes scaling of the energy levels so that the spacing between levels $^1S^e(K=N-1)$ and $^1P^o(K=N-2)$ appears the same in each shell. $N$ dependence of spacings will be described in Sec. IV D. These regular progressions and near-degeneracies are quite striking; they are certainly not what one expects to find in a problem which is supposed to be nonseparable. The near-degeneracies in these

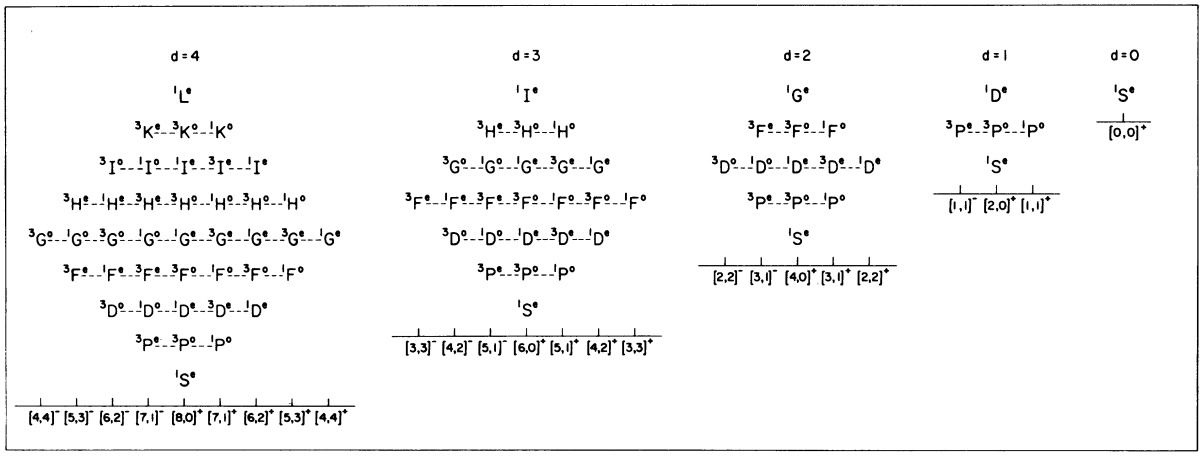


FIG. 4. $d$-supermultiplet classification of term symbols for intrashell doubly excited states with $d\leq 4$, where for each shell $d=0,1,\ldots,N-1$. O(4) multiplets $[P,T]^\pm$ containing terms with $L=T,T+1,\ldots,P$ are seen vertically within $d$ supermultiplets. The lines between terms with the same $L$ are used to identify similar levels in the energy spectra.

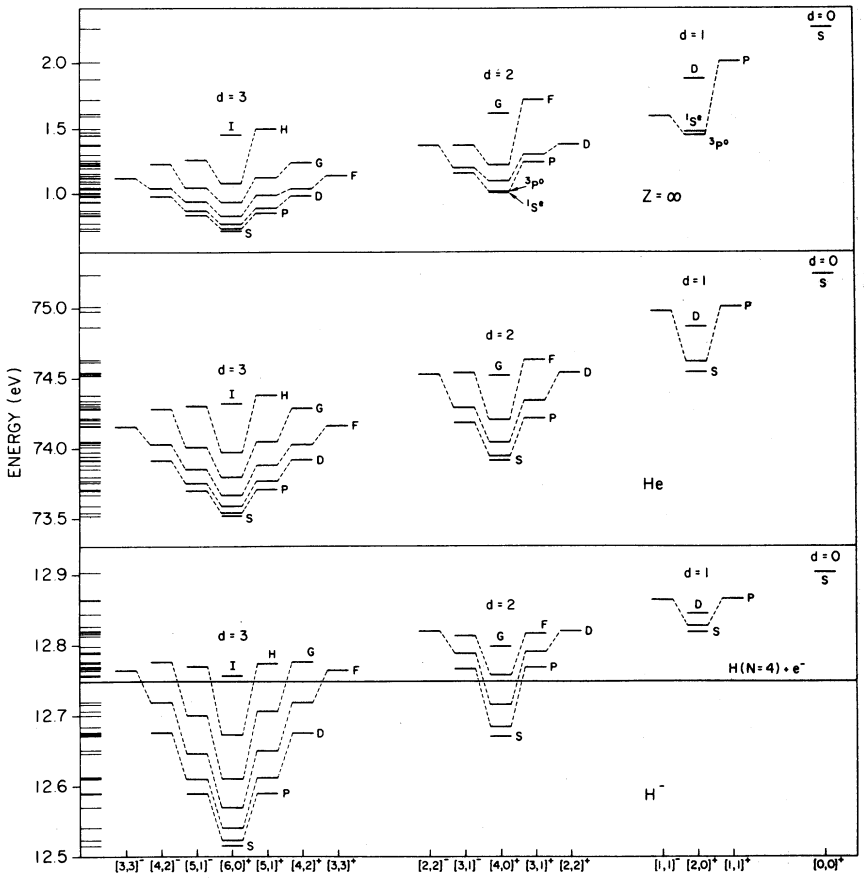


FIG. 5. $d$-supermultiplet classification of computed intrashell spectra for $N=4$ levels in $H^-$, He, and $Z=\infty$ (hydrogenic); these are the same levels shown earlier in Fig. 3 with $I$ supermultiplets. Term symbols for levels were shown in Fig. 4.

largest diamond supermultiplets ($I=0$) display slight weakening with increasing $N$ for $K=0$; states with higher values of $T$ lie slightly lower in energy.

The complete $d$-supermultiplet spectra for intrashell energy levels $2 \leq N \leq 5$ are shown in Fig. 7 for He, and in Fig. 8 for $H^-$. The breaks in energy scale between $N=2$ and 3 and between $N=3$ and 4 are required so that we can show the small rotational spacings of levels at higher $N$. There is no break in scale between $N=4$ and $N=5$. The most striking feature of these figures is the near constancy of the shape of supermultiplets with the same value of $d$ in different shells. Analysis of autoionization widths for levels $N=2$ and $N=3$ in He shows a similar trend, but we do not know if this extends to higher shells. In addition to our own computed levels for $N=2$, we have also displayed other, more accurate experimental and theoretical results.[11,28] Although individual levels show some differences, overall the shapes of the supermultiplets are quite similar.

In Fig. 8 we have again included levels above threshold, keeping in mind that an interpretation of these levels as resonances in $H^-$ is questionable. One reason for showing them here is to illustrate how these instabilities are related to the ro-vibrational progressions of levels. Vertical excitation within a $d$ supermultiplet puts some of the levels above threshold in $H^-$; this is analogous to rotational predissociation in a molecule, where the centrifugal barrier due to rotation pushes otherwise stable states above the dissociation limit. Here we also see an apparent vibrational instability with increasing $T$ in a $d$ supermultiplet, decreasing $d$ between $d$ supermultiplets, or decreasing $K$ in an $I$ supermultiplet (cf. Fig. 6). There does not appear to be a simple rule with the quantum numbers that would describe which levels lie below threshold in each shell, and also which levels would have the greatest stability above threshold as quasibound shape resonances. The usual criterion for predicting which $H^-$ channels support intershell series below threshold is that the centrifugal parameter in Eq. (3.28) describe a long-range attraction: $A < -\frac{1}{4}$. Here we are interested in channels which satisfy this criterion and

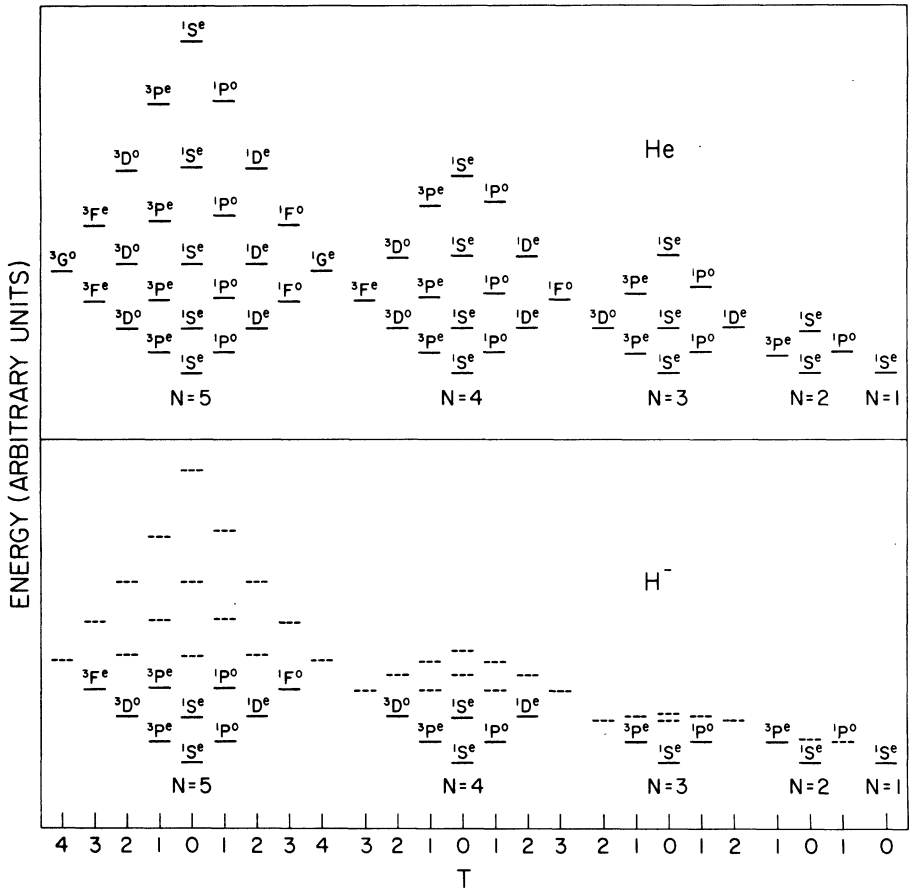


FIG. 6. Illustration of largest diamond supermultiplets ($I=0$) for each shell $N \leq 5$, showing the pattern of approximate near-degeneracies; levels in each of these diamonds have $L=T$. Note the "collapse" of levels above each threshold in $H^-$, indicated by the dashed lines, due to a variational instability. This collapse weakens with increasing $N$, due to the cutoff $n \leq 7$ in the radial basis. A more marked collapse was found for $S$ and $P$ levels when $n \leq 10$, but these calculations were not extended to include all values of $L$ and hence are not displayed here.

also support intrashell levels. Herrick has described some of the properties of the eigenspectrum of the channel invariant $\hat{A}$ in terms of the $K, T$ classification for lower values of $N$ (Ref. 15). It is interesting to note that the channel $K=N-1$, $T=0$ gives $A<-\frac{1}{4}$ only for the following values of the angular momentum: $0 \leq L \leq 2N-2$, at least for $N \leq 5$. This is the same cutoff as was seen for intrashell $L$ in the O(4) shell theory, since these values of $K$ and $T$ correspond to the intrashell multiplet $[2N-2, 0]^+$. This is the multiplet whose levels look most like those of a rigid rotor,[27] and may be seen as the central multiplet in the largest $d$ supermuliplet of each shell in Fig. 8. Values of the centrifugal parameter $A$ for the highest intrashell levels (i.e., $L=2N-2$) in these rotorlike series are the following: $-0.81(^1D^e, N=2)$, $-2.56(^1G^e, N=3)$, $-5.23(^1I^e, N=4)$, and $-8.82(^1L^e, N=5)$. These values are sufficiently negative so that accurate variational calculations with the charge wave function $\Psi_N$ should give bound anion states below each threshold. Note, however, that our calculations give the $^1I^e$ and $^1L^e$ levels for $N=4$ and 5, respectively, above threshold. We attribute this to radial inflexibility in the linear approximation of $\Psi_N$, which becomes less accurate for higher shells, due to the cutoff $n \leq 7$ in our hydrogenic radial basis. We have carried out calculations for $S$ and $P$ levels using an extended radial basis $N \leq n \leq 10$, and find that many of the $H^-$ levels collapse dramatically toward threshold as expected. However, some of the levels near threshold are very insensitive to changes in the linear configuration basis. This behavior is a possible indication of shape resonances, but more accurate calculations are needed.

### D. Scaling laws for computed ro-vibration levels

A detailed investigation of the similarities between the present supermultiplets and molecular

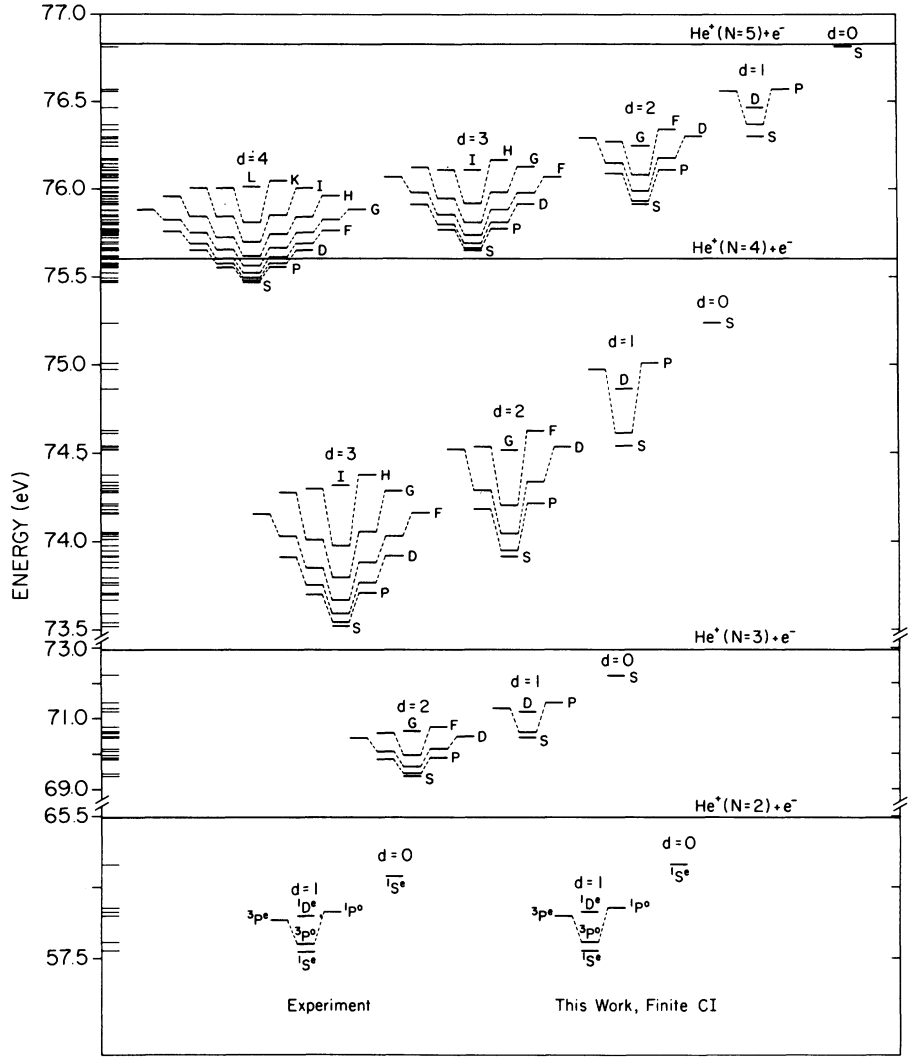


FIG. 7. *d*-supermultiplet classification of all computed intrashell double-excitation levels $2 \leq N \leq 5$ for He; the unresolved spectrum is shown at the left. Other energies from Refs. 11 and 28 are included for $N=2$, for comparison with the present hydrogenic configuration interaction results. Term symbols for the supermultiplets were illustrated in Fig. 4.

ro-vibration levels will be given in Ref. 2. Here we will use only a very simple ro-vibrational picture in order to interpret the qualitative behavior of our computed level spacings for increasing $N$. We find results entirely consistent with the behavior of ro-vibrational energy parameters for increasing shell size.

If we include only rigid rotations and harmonic bending vibrations, the intrashell levels are described by the formula[1]

$$E = B_e [L(L+1) - T^2] + \omega_2 (v+1), \tag{4.5}$$

where $B_e$ is the equilibrium rotational constant, $\omega_2$ is the vibrational bending constant, and $v = N - 1 - K$ is the integer quantum number for a two-dimensional oscillator. The first rotational excitation energy described by Eq. (4.5) for $^1S^e \rightarrow {}^3P^o$ is $2B_e$. We take the first vibrationlike excitation $^1S^e \rightarrow \bar{P}$ as $\omega_2 + B_e$, where $\bar{P}$ denotes the average of the state $^1P^o$ and $^3P^e$. Notice that the vibrational excitation includes a contribution $B_e$ from the excitation of vibrational angular momentum.

A simple power-law fit of ro-vibrational parameters from our computed spectra for levels $N \leq 5$ gives the following dependence on $N$ in He:

$$B_e = 0.169\, N^{-4.38}, \quad \omega_2 = 0.692\, N^{-3.38}, \tag{4.6}$$

and in $H^-$:

$$B_e = 0.058\, N^{-4.29}, \quad \omega_2 = 0.234\, N^{-3.25}, \tag{4.7}$$

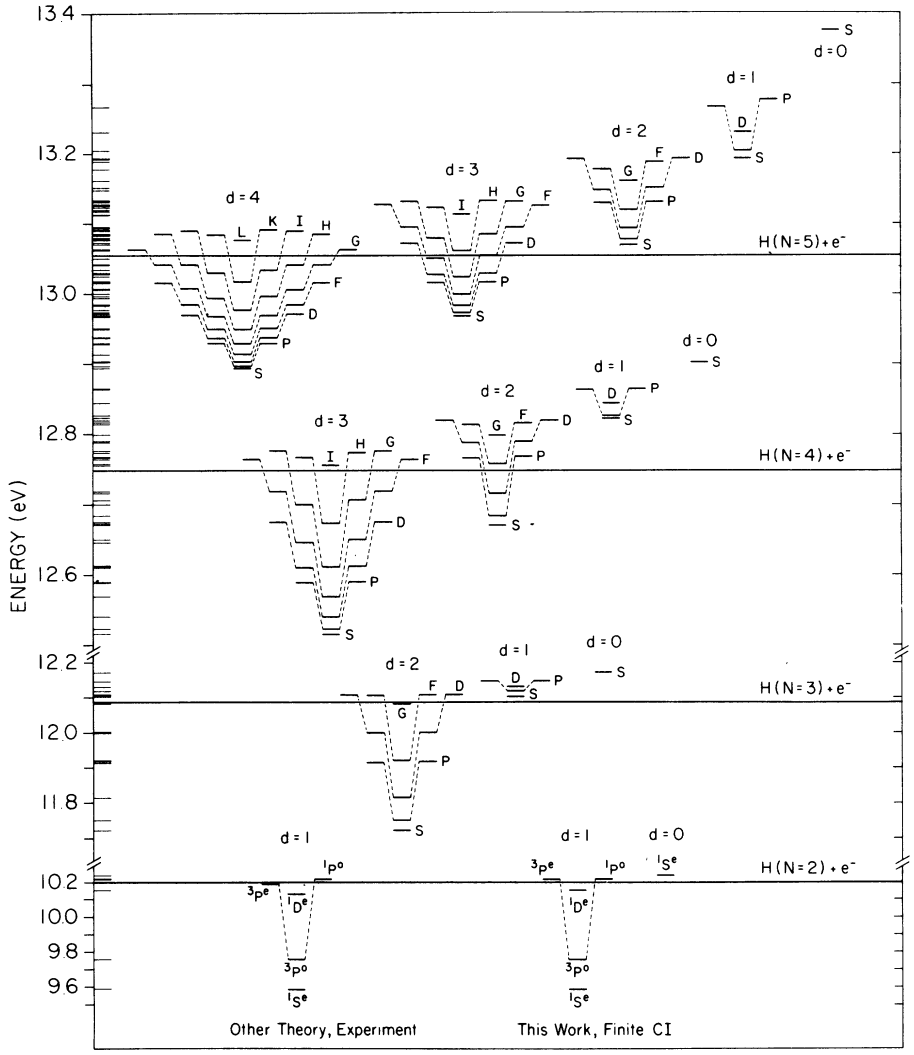


FIG. 8. $d$-supermultiplet classification of all computed intrashell double-excitation levels $2 \leq N \leq 5$ for $H^-$; the unresolved spectrum is shown at the left. Other energies from Refs. 11 and 28 are included for $N=2$, for comparison with the present hydrogenic configuration interaction results. Term symbols for the supermultiplets were illustrated in Fig. 4. A discussion of energy eigenvalues appearing above each threshold is given in Secs. II and IV of the text.

where we have used atomic units. These results indicate that the rotationlike level spacing decreases faster than the vibrationlike spacing, and suggest increasing approximate separability of the energies at higher $N$. This behavior is seen clearly in Figs. 7 and 8. The separability is much less than what is found in molecular spectra, where, for example, $\omega_2/B_e = 1720$ for $CO_2$. A similar value would be obtained from Eqs.(4.6) and (4.7) when $N \simeq 400$.

The empirical scaling laws are reasonably consistent with a simple model of the atom as a rotor-vibrator. First, we note that ro-vibrationlike spacings in Figs. 7 and 8 are much smaller than energies between neighboring shells, indicating that collective intrashell motions of electrons are slower than radial motions which account for the atomic shell structure. For the sake of simplicity, let us assume the intrashell correlation in low-lying levels is described with electrons on the surface of a spherical shell. The nucleus is fixed at the center, and the sphere radius $R$ corresponds roughly to the region of peak radial probability in the wave function. A linear $XYX$ molecular configuration for the electrons ($X$) and nucleus ($Y$) is consistent with a minimum in the angular part of the Coulomb repulsion between two electrons at $\theta_{12} = 180°$. Analysis of the ro-vibrational parameters for this model shows the following dependence on shell radius[2]:

$$B_e \propto R^{-2}, \quad \omega_2 \propto R^{-1.5}. \tag{4.8}$$

Note in particular that these constants predict a faster dropoff of rotational spacings than vibrational spacings with increasing shell size. This is consistent with the empirical results for doubly excited atoms, where increasing $N$ corresponds to a larger shell radius. The average radius of a spherical hydrogen atom, for example, is $\bar{r} = 1.5 N^2$ in atomic units. If this same scaling continued to apply in the case of two-electron atoms, Eq. (4.8) would predict $B_e \propto N^{-4}$ and $\omega_2 \propto N^{-3}$, which agree qualitatively with the computed ones for He and $H^-$. The scaling laws described in Eqs. (4.6) and (4.7) suggest an effective-double-excitation shell radius which scales as $R \propto N^{2.2}$. It would be extremely useful to have more accurate scaling laws in the region of very high $N$, since analytic continuation of the rotor-vibrator wave function above threshold would give a simple model for angular distributions of two electrons leaving the atom at an equilibrium angle of $\theta_{12} = 180°$.

The preceding ro-vibrational interpretation is pleasing because it lends support to the picture of the doubly excited atom as a linear rotor-vibrator. We now give an O(4) interpretation of the model which indicates that the molecular picture and the group theoretical one are not incompatible. The molecular approach assumed harmonic bending of the $XYX$ structure about the linear equilibrium configuration. Here we will assume the following Hamiltonian for the ro-vibrational energy:

$$\hat{\epsilon} = (\vec{l}_1^{\,2} + \vec{l}_2^{\,2})/2R^2 + (1 + \cos\theta_{12})/8R. \tag{4.9}$$

The first term represents the centrifugal part of the kinetic energy; the second term describes the leading-order dipole portion of the operator $1/r_{12}$. The potential energy term reduces to the harmonic potential near $\theta_{12} = 180°$. Our goal is to diagonalize the energy using a representation of O(4) defined on angular functions only, with one-electron orbital angular momentum $0 \leq l \leq N-1$ for each atomic shell. Since we are concerned only with the lowest energy eigenvalues in each shell, we can represent matrix elements of the dipole unit vector $\hat{r}$ for each electron with the O(4) generator $\vec{b}/N$. This substitution is not exact, but gives a good approximation of matrix elements when the condition $l \ll N$ is satisfied.[15] We therefore replace the energy operator $\hat{\epsilon}$ in Eq. (4.9) with the following modified O(4) energy operator for the shell model:

$$\hat{\epsilon}_0 = (\vec{l}_1^{\,2} + \vec{l}_2^{\,2})/2R^2 + (\vec{b}_1 \cdot \vec{b}_2)/8RN^2 + 1/8R. \tag{4.10}$$

Eigenvalues of this energy operator could be found at each value of the radius $R$ by numerical diagonalization of the intrashell energy matrix. Our concern here is with values of $R$ where O(4) can be used to achieve this diagonalization. We identify two radii where this can be done for each value of $N$.

The first O(4) interpretation of the intrashell energy is seen when $R \to 0$ in which case the centrifugal term dominates the energy. In this regime the energies are described by eigenvalues of the Casimir invariant $\vec{L}^2 + \vec{D}^2 = p(p+2) + q^2$ for the group $O(4)_D$ which we described in Sec. III. The connection is seen in the fact that $\vec{l}_1^{\,2} + \vec{l}_2^{\,2} = \frac{1}{2}(\vec{L}^2 + \vec{D}^2)$. The eigenstates are single configuration states as described in Eq. (3.11).

The $O(4)_D$ symmetry is broken at higher values of $R$ when the dipole coupling becomes important. Recall that values of the shell radius $R \simeq N^2$ are most typical of the doubly excited atoms, which generally involve substantial configuration mixing in the wave function in order to account for the electron correlation. It is of considerable interest then, that we find that the second intrashell group $O(4)_B$ gives an exact diagonalization of the energy when $R = 8N^2$. We call this the "O(4) shell limit" of the model. The energy is described by Casimir invariants of the subgroup chain $O(4)_B \supset O(3)$, and has the following form on the O(4) shell only:

$$\hat{\epsilon}_0 = (4N^2 - 2 - \vec{B}^2)/128N^4. \tag{4.11}$$

Recall that $\vec{B}^2$ is diagonal in the coupled representation of Eq. (3.12), and has eigenvalues $\vec{B}^2 = P(P+2) - [L(L+1) - T^2]$ which we have written in a form that emphasizes a symmetric top form of the rotational energy. The "vibrational" energy is identified with the correspondence $P = 2N - 2 - v$ between O(4) and vibrational quantum numbers. This leads to the following ro-vibrational parameters predicted by the model in the O(4) shell limit:

$$B_e = \tfrac{1}{128}N^{-4}, \quad \omega_2 = \tfrac{1}{32}N^{-3}. \tag{4.12}$$

Scaling properties of these O(4) constants are consistent with the empirical values we found for He and $H^-$. However, the magnitudes are too small to account for the actual level spacings in our computed spectra for He and $H^-$, evidently due to a smaller value of $R$ for these systems. The O(4) shell radius is therefore unphysical and describes a highly idealized model. The larger value of $R$ is more typical of a system involving a fractional charge $Z < 1$. The central Coulomb field for electrons in the linear configuration $\theta_{12} = 180°$ is attractive only when $Z > \frac{1}{4}$.

Although the O(4) model predicts constants that are too small, it does give a very interesting prediction of the relative separation of the rotationlike and vibrationlike energy contributions. This is described by a coefficient $\gamma = N(B_e/\omega_2)$, which includes a factor $N$ to account for the different scal-

ing of rotation and vibration energy. The O(4) shell model described above predicts $\gamma = 0.25$, independent of $N$. Our computed energy spectra for He and $H^-$ also show a rather surprising degree of constancy:

$$\gamma_{He} = 0.243 \pm 0.001 \quad (N = 2-5)$$
$$\gamma_{H^-} = 0.233 \pm 0.005 \quad (N = 3-5). \tag{4.13}$$

The value for the $N = 2$ shell of $H^-$ is slightly larger, $\gamma = 0.321$. We are impressed by the closeness of these values, and their agreement with the value 0.25 for the O(4) model.

## V. SUMMARY

We have investigated three aspects of intrashell doubly excited states of two-electron atoms, thereby providing new insight to the supermultiplet classification proposed in Ref. 1. First, we have extended earlier theoretical calculations to include for the first time all intrashell levels $N \leq 5$ in He and $H^-$. This study included all possible intrashell terms $0 \leq L \leq 2N-2$ necessary to construct the complete supermultiplet spectrum. Because energy differences play an important role in the ro-vibrational interpretation of supermultiplets, we have been careful to adopt a systematic computational procedure for all states. The present variational estimates of energies were carried out in the framework of a "charge wave function" approach[6] for the nonclosed-shell electron correlation in doubly excited states. The second part of our investigation was the classification of intrashell levels according to O(4). Earlier work in this area had focused on either the classification of intrashell configuration mixing at high $Z$, or channel mixing at low $Z$. As Ref. 1 noted, the two views lead to two hierarchies of quantum numbers, and hence two types of supermultiplets for intrashell levels. Our present work has provided a much clearer picture of the rotationlike and vibrationlike aspects of the electron correlation implicit in the O(4) approaches. These interpretations were made possible by our study of Lie-algebra generators, and our derivation of matrix elements for intrashell operators (cf. Appendix) using three different intrashell O(4) groups. The third part of our investigation was the supermultiplet classification of the spectra for He and $H^-$. As described in Ref. 1, the supermultiplets are built up from different O(4) levels, and thus encompass a much broader, and richer range of spectral systematics than could have otherwise been expected. The unresolved double-excitation spectra are very complicated, and we have found many example of level clustering between states of different $L$. The supermultiplets are found to give a very efficient resolution of the entire intrashell spectrum, including the ro-vibrational structure and accidental near-degeneracies that other, more limited classification methods have failed to recognize. We illustrated the power of our supermultiplets for uncovering these novel spectral features in some detail for the $N = 4$ shell, and then very generally for all double-excitation shells $N \leq 5$. It seems quite clear from these results what could be expected for supermultiplets in even higher shells. It would be extremely useful then, to have more accurate estimates of the supermultiplet energies and scaling. These would also shed light on the question of possible shape resonances above higher thresholds in $H^-$. Our present investigation of scaling of low-lying ro-vibrational excitation energies is at least qualitatively consistent with a picture of rotational and bending mode vibrational collective motion for the intrashell electron correlation. As we discussed in Sec. III, this interpretation may possibly be linked to coupled rotations and vibrations of Lenz vectors at high $Z$. However, this view is only approximate, and does not explain why the ro-vibrational freatures seem to become sharper at low values of $Z$. We will investigate a ro-vibrational interpretation of the two-electron Hamiltonian more carefully in a subsequent paper.[2]

It is clear that additional mathematical properties of the supermultiplets need to be identified, and exploited in the form of approximate energy level formulas that can be extrapolated to higher $N$. Our present results provide considerable semiempirical evidence for an approximate separability that has thus far eluded identification. In summary then, we have found the supermultiplet approach to be an extremely efficient way of unravelling double-excitation spectra. Our analysis of computed ro-vibrational structure in these spectra has allowed us to accomplish better what has long been difficult to do: Give a simple physical picture of the electron correlation in doubly excited states.

## ACKNOWLEDGMENTS

This research was supported by NSF Grants Nos. CHE 761 033 2 and CHE 790 950 0. Acknowedgement is made to the Donors of the Petroleum Research Fund, administered by the American Chemical Society, for partial support of this research. One of the authors (D.R.H.) would like to thank the Camille and Henry Dreyfus Foundation for financial support.

## APPENDIX: $SO(4)_1 \times SO(4)_2$ MODEL OF INTRASHELL SPLITTING

The purpose of this section is twofold. First, we derive some useful matrix elements involving

Casimir invariants of the three O(4) groups defined in Sec. III; these results lead directly to Eq. (3.31) for the average value of $\cos\theta_{12}$ in the intrashell hydrogenic basis. They are also useful for decribing matrix elements of the intrashell model energy $\epsilon_0$ in Sec. IV. The second point we consider is the general form of energy-level splitting for the intrashell states, under the assumption that this is a simple function of Casimir invariants for the chain $SO(4)_1 \times SO(4)_2 \supset SO(4)_B \supset SO(3)$.

We start by considering matrix elements of an operator

$$\Lambda = \sum_{i,j=1}^{12} c_{ij} Y_i Y_j , \tag{A1}$$

with $Y_i$ denoting Lie-algebra generators of the intrashell $SO(4)_1 \times SO(4)_2$, and with real coefficients $c_{ij}$. We consider only forms for $\Lambda$ that are symmetric with respect to the permutation-inversion-rotation symmetry for two-electron atoms. This reduces the number of independent parameters in Eq. (A1) to four, and $\Lambda$ is a linear combination of the operators $\vec{L}^2$, $\vec{B}^2$, $\vec{D}^2$, and $\vec{A}^2$. When working in the basis $|PQLM)$ for the group $SO(4)_B$, it is convenient to express $\Lambda$ with four parameters $\alpha$, $\beta$, $\gamma$, and $\delta$ in the form

$$\Lambda = \alpha(\vec{L}^2 + \vec{B}^2 + \vec{D}^2 + \vec{A}^2) + \beta(\vec{L}^2 + \vec{B}^2) + \gamma\vec{L}^2 + \delta(\vec{D}^2 - \vec{A}^2) . \tag{A2}$$

The first three terms in this expression are Casimir invariants from the chain $SO(4)_1 \times SO(4)_2 \supset SO(4)_B \supset SO(3)$, and for intrashell states they are given by

$$\begin{aligned} &\vec{L}^2 + \vec{B}^2 + \vec{D}^2 + \vec{A}^2 = 4N^2 - 4 , \\ &\vec{L}^2 + \vec{B}^2 = P(P+2) + Q^2 , \\ &\vec{L}^2 = L(L+1) . \end{aligned} \tag{A3}$$

The fourth term in Eq. (A2) breaks the $SO(4)_B$ symmetry in a different way; it has nonzero matrix elements between different irreducible representations $(P, Q) \leftrightarrow (P', Q')$. Thus $\delta$ represents an asymmetry parameter for the interaction $\vec{D}^2 - \vec{A}^2$. This asymmetry is analogous to the asymmetry term $J_x^2 - J_y^2$ in the energy formula for a three-dimensional top: $\epsilon = aJ^2 + bJ_z^2 + c(J_x^2 - J_y^2)$. The symmetric top energy is seen from this when $c = 0$; the analogous situation in the operator $\Lambda$ occurs when $\delta = 0$, in which case $\Lambda$ is diagonal on the basis $|PQLM)$.

As indicated in Eq. (A3), the matrix elements of $\vec{A}^2$ and $\vec{D}^2$ are not independent. Furthermore, it is straightforward to see from the expansion formulas in Eqs. (3.12)–(3.14), that the matrix elements of the Casimir invariant $\vec{L}^2 + \vec{A}^2$ for $SO(4)_A$ are related to those of the invariant $\vec{L}^2 + \vec{D}^2$ for $SO(4)_D$ by a simple phase factor:

$$(P'Q'LM|\vec{L}^2 + \vec{A}^2|PQLM) = (-1)^{c+c'}(P'Q'LM|\vec{L}^2 + \vec{D}^2|PQLM) , \tag{A4}$$

with $c = N - 1 - \frac{1}{2}(P - Q)$. Combining Eqs. (A3) and (A4), we find the expression

$$(P'Q'LM|\vec{L}^2 + \vec{D}^2|PQLM)[1 + (-1)^{c+c'}] = \delta_{PP'}\delta_{QQ'}[4N^2 - 4 + \vec{L}^2 - \vec{B}^2] . \tag{A5}$$

Here $\delta_{ij} = 1$ if $i = j$, and $\delta_{ij} = 0$ if $i \neq j$. Eigenvalues of $\vec{L}^2$ and $\vec{B}^2$ are understood on the right-hand side of Eq. (A5), and following equations. Our main interest lies with the diagonal matrix elements $P' = P$, $Q' = Q$. However, it is interesting to note the selection rule that off-diagonal matrix elements of $L^2 + D^2$, and hence also $D^2$ and $A^2$, vanish identically when $c + c'$ or $c - c'$ is an even integer; that is, they vanish when either $\Delta P$ or $\Delta Q$ is nonzero, and $\frac{1}{2}(\Delta P - \Delta Q)$ is even.

We now use Eq. (A5) in order to evaluate diagonal matrix elements of the operators $\vec{l}_1^2 + \vec{l}_2^2 = \frac{1}{2}(\vec{L}^2 + \vec{D}^2)$ and $2\vec{b}_1 \cdot \vec{b}_2 = 2N^2 - 2 - \vec{B}^2 - \frac{1}{2}(\vec{L}^2 + \vec{D}^2)$, which represent special cases of the operator $\Lambda$. These are easily evaluated as

$$(PQLM|\vec{l}_1^2 + \vec{l}_2^2|PQLM) = N^2 - 1 + \tfrac{1}{4}(\vec{L}^2 - \vec{B}^2) , \tag{A6}$$

$$(PQLM|2\vec{b}_1 \cdot \vec{b}_2|PQLM) = N^2 - 1 - \tfrac{1}{4}(\vec{L}^2 + 3\vec{B}^2) . \tag{A7}$$

These results have not been described in previous work for doubly excited states. Suitable combinations of Eqs. (A6) and (A7) lead directly to diagonal matrix elements of the energy $\epsilon_0$ in Eq. (4.12). We can also use Eq. (A7) in order to evaluate average values of $\cos\theta_{12}$ for hydrogenic intrashell states, using the operator replacement $\cos\theta_{12} \to (\vec{b}_1 \cdot \vec{b}_2)/N^2$; the results of this were displayed in Eq. (3.31). We derive another useful result using the operator replacement $\vec{r}_1 \cdot \vec{r}_2 \to (3N/Z)^2(\vec{b}_1 \cdot \vec{b}_2)$ on the hydrogenic intrashell basis; in terms of this we evaluate an expression for the mean-square interelectronic separation,

$$(PQLM|r_{12}^2|PQLM) = (N/4Z)^2(20N^2 + 76 + 33\vec{B}^2 + 3\vec{L}^2) . \tag{A8}$$

One sees explicitly in this formula that, for each value of $L$, the electron correlation is more favorable in SO(4) states which correspond to larger values of $\vec{B}^2$. Wulfman[13] described an approximate formula for diagonal matrix elements of the Coulomb repulsion operator $1/r_{12}$ in the hydrogenic intrashell basis. However, he did not evaluate contributions of a term $\vec{l}_1^2 + \vec{l}_2^2$ in his formula. We can now account for this term using Eq. (A6) derived here; in terms of this we find that Wulfman's formula becomes simply[29]

$$(PQLM|1/r_{12}|PQLM)$$
$$\simeq(4Z/N)(24N^2+24+14\vec{B}^2+2\vec{L}^2)^{-1/2}. \quad \text{(A9)}$$

The preceding results agree qualitatively with the level orderings found *at low Z* in the isoelectronic series for two-electron atoms. In view of the relatively small $T$ doubling for many intrashell states, it is reasonable to assume that the energy in each level involves intrashell splitting that is a simple function of $\Lambda$ when $\delta=0$. In this case the energy-level ordering for each shell would be a function of the operator

$$X=\vec{B}^2+\lambda\vec{L}^2, \quad \text{(A10)}$$

where $\lambda$ is a parameter for the $SO(4)_B \supset SO(3)$ symmetry breaking. Sinanoğlu and Herrick described approximate empirical formulas for intrashell energies.[12] In the case of He they found the parameter $\lambda\simeq\frac{1}{10}$. This empirical value is similar to $\lambda=\frac{1}{11}$ from Eq. (A8) for the hydrogenic mean-square correlation, and the value $\lambda=\frac{1}{7}$ from our version Eq. (A9) or Wulfman's approximation of the repulsion energy at high $Z$.

Although the operators $\Lambda$ and $X$ can account for many of the qualitative features of the intrashell spectra, it is clear that more accurate energy formulas are needed. We note, for example, that diagonal matrix elements of $\Lambda$ cannot describe an exact degeneracy for levels in the largest diamond supermultiplet in each shell. In this sense the near-degeneracies in the computed $I$ supermultiplets are still "accidental" from the group theoretical approach to the problem. This contrasts with the molecular ro-vibrational approach, where the near-degeneracy is part of the degeneracy of a two-dimensional oscillator.[1,2] The best description of these computed near-degeneracies with $X$ is found when the parameter $\lambda=0$. In this case the angular momentum contribution to the energy is a function of $L(L+1)-T^2$, and is thus similar to the symmetric top energy for a rotor vibrator.

---

*Present address: Chemistry Department, Columbia University, New York, N. Y. 10027.

[1]D. R. Herrick and M. E. Kellman, Phys. Rev. A 21, 418 (1980).

[2]M. E. Kellman and D. R. Herrick, Phys. Rev. A 22, 1536 (1980).

[3]Spectroscopic symbols for higher angular momentum states are $S, P, D, F, G, H, I, K, L, \ldots$ for $L=0,1,2,3,4,5,6,7,8,\ldots$; the parity is even (e) or odd (o).

[4]U. Fano, Phys. Today 29:9, 32 (1976); and references therein.

[5]D. R. Herrick, J. Chem. Phys. 67, 5406 (1977).

[6]O. Sinanoğlu, in *Atomic Physics*, edited by B. Bederson, V. W. Cohen, and F. M. J. Pichanick (Plenum, New York, 1969); W. L. Luken and O. Sinanoğlu, At. Data Nucl. Data Tables 18, 525 (1976).

[7]P. G. Burke and D. D. Mc Vicar, Proc. Phys. Soc. London 86, 989 (1965).

[8]R. S. Oberoi, J. Phys. B 5, 1120 (1972).

[9]D. R. Herrick and O. Sinanoğlu, Phys. Rev. A 11, 97 (1975).

[10]L. Lipsky, R. Anania, and M. J. Conneely, At. Data Nucl. Data Tables 20, 127 (1977).

[11](a) G. J. Schulz, Rev. Mod. Phys. 45, 378 (1973); (b) H. C. Bryant *et al.*, Phys. Rev. Lett. 38, 228 (1977); (c) D. E. Golden, Adv. At. Mol. Phys. 14, 1 (1978).

[12]O. Sinanoğlu and D. R. Herrick, J. Chem. Phys. 62, 886 (1975); 65, 860(E) (1976); Chem. Phys. Lett. 31, 373 (1975).

[13]C. Wulfman, Chem. Phys. Lett. 23, 370 (1973).

[14]D. R. Herrick, J. Math. Phys. 16, 1047 (1975).

[15]D. R. Herrick, Phys. Rev. A 12, 413 (1975); 17, 1 (1978).

[16]S. I. Nikitin and V. N. Ostrovsky, J. Phys. B 9, 3141 (1976); 11, 1681 (1978).

[17]L. C. Biedenharn, J. Math. Phys. 2, 433 (1961).

[18]V. Fock, Z. Phys. 98, 145 (1935).

[19]V. Bargmann, Z. Phys. 99, 576 (1936).

[20]Other literature for hydrogen SO(4) is too extensive to give here, and may be found in M. J. Englefield, *Group Theory and the Coulomb Problem* (Wiley, New York, 1972).

[21]W. Pauli, Z. Phys. 36, 336 (1926).

[22](a) C. Wulfman, Phys. Lett. A 26, 397 (1968); (b) J. Alper and O. Sinanoğlu, Phys. Rev. 177, 77 (1969).

[23]D. R. Herrick and M. E. Kellman, Phys. Rev. A 18, 1770 (1978).

[24]E. U. Condon and G. H. Shortley, *Theory of Atomic Spectra* (Cambridge University Press, Cambridge, England, 1967).

[25](a) P. G. Burke, Adv. At. Mol. Phys. 4, 173 (1968); (b) J. Macek and P. G. Burke, Proc. Phys. Soc. London 92, 351 (1967).

[26]P. Rehmus, M. E. Kellman, and R. S. Berry, Chem. Phys. 31, 239 (1978).

[27]M. E. Kellman and D. R. Herrick, J. Phys. B 11, L755 (1978).

[28](a) W. C. Martin, J. Phys. Chem. Ref. Data 2, 257 (1973); (b) S. Bashkin and J. O. Stoner, Jr., *Atomic Energy Levels & Grotrian Diagrams* (North-Holland, Amsterdam, 1975), Vol. 1, p. 10; (c) J. S. Risley, A. K. Edwards, and R. Geballe, Phys. Rev. A 9, 1115 (1974). (Note: The level they call $2s2p\ ^1P^o$ at 10.18 eV is found to be $2s3p$ with $K=1$, $T=0$ in our O(4) classification; our $2s2p$ level is found above threshold at 10.218 eV with $K=0$, $T=1$, using a Rydberg constant $R_H=13.59842$ eV.)

[29]This formula is found to predict some curious accidental degeneracies for some of the SO(4) levels. However, these degeneracies do not appear to be part of the actual spectrum of $1/r_{12}$, or of He and $H^-$ spectra.